JOC Article

Cholic Acid Derivatives Containing Both 2-Naphthylcarbamate and 3,5-Dinitrophenylcarbamate Groups: A Combined Circular Dichroism−Molecular Mechanics Approach to the Definition of Their Molecular Conformation

Giuliano Alagona,[†] Caterina Ghio,[†] Anna Iuliano,*[,‡] Susanna Monti,*[,†] Ilaria Pieraccini,[‡] and Piero Salvadori[‡]

CNR-IPCF, Istituto per i Processi Chimico-Fisici, Molecular Modeling Laboratory, Via Moruzzi 1, I-56124 Pisa, Italy, and Dipartimento di Chimica e Chimica Industriale, Università di Pisa, Via Risorgimento 35, I-56126 Pisa, Italy

iuliano@dcci.unipi.it; s.monti@ipcf.cnr.it

Received November 21, 2002

CD spectra of the chiral auxiliaries for enantioselective HPLC *N*-allyl-*N*′-methyl-3,12-bis(2-naphthyl)carbamoyloxy-7-(3,5-dinitrophenyl)carbamoyloxycholan-24-amide (**1**), *N*-allyl-*N*′-methyl-3-(3,5-dinitrophenyl)carbamoyloxy-7,12-bis(2-naphthyl)carbamoyloxycholan-24-amide (**2**), *N*-allyl-*N*′-methyl-3,7-bis(2-naphthyl)carbamoyloxy-12-(3,5-dinitrophenyl)carbamoyloxycholan-24-amide (**3**), and *N*-allyl-*N*′-methyl-3,7,12-tris(2-naphthyl)carbamoyloxycholan-24-amide (**4**) are presented. To determine the preferred conformations of those chiral auxiliaries, a random search based on the aromatic side-chain conformational degrees of freedom was performed and the energy was minimized using two different molecular mechanics force fields. The low energy structures presenting common features were arranged in groups and selected exploiting appropriate filters. The calculation of theoretical CD spectra according to the De Voe model has allowed a further discrimination among the conformations, specifying which of them gave calculated CD spectra in acceptable agreement with the experimental ones. Finally, taking into account the additivity of the contributions of each 2-naphthylcarbamate chromophore to the CD spectrum of the cholic acid derivatives, and, hence, choosing, for derivatives **1**−**3**, those conformations in which the 2-naphthylcarbamate groups take a similar disposition as in **4**, the preferentially assumed conformation of each compound was obtained. A molecular dynamics simulation in the presence of acetonitrile allowed the fluctuations of one of the structures, used as a test case, depending on environmental effects, to be examined.

Introduction

The use of bile acids in chiral recognition processes has received a great deal of attention in the past decade. These natural products, because of their unique structure endowed with several functional groups arranged in a rigid chiral backbone, have successfully been used in the construction of extended preorganized molecular architectures.[1] In addition, their enantiodiscriminating properties can be suitably tuned by reacting the original functional groups present in the parent compound with appropriate derivatizing agents. In this way, chiral auxiliaries for asymmetric Diels−Alder reactions[2] or for asymmetric couplings,[3] as well as systems for the enantioselective extraction of amino acids[4] or molecular tweezers,[5] have been obtained.

More recently, attention has been paid to the use of bile acids in enantioselective HPLC: both underivatized[6] and derivatized[7] bile acids have been linked to silica gel and used as chiral stationary phases (CSPs) for the HPLC resolution of racemic compounds. In this framework, we recently demonstrated that bile acids possessing both π-acceptor and π-donor aromatic moieties behave as biselector systems in enantioselective HPLC, the corresponding CSPs being able to resolve racemic compounds having π-donor character as well as chiral compounds possessing π-acceptor aromatic groups.[8] Among these CSPs, those obtained starting from the cholic acid derivatives **1**−**4** (Figure 1) resulted very promising

* To whom correspondence should be addressed. (A.I) Phone: +39-050-918232. Fax: +39-050-918260. (S.M.) Phone: +39-050-3152520. Fax: +39-050-3152442.

[†] CNR-IPCF.

[‡] Università di Pisa.

(1) Davis, A. P. *Chem. Soc. Rev*. **1993**, *22*, 243−253.

(2) (a) Maitra, U.; Mathivanan, P. *J. Chem. Soc., Chem. Commun*. **1993**, 1469−1471. (b) Mathivanan, P.; Maitra, U. *J. Org. Chem*. **1995**, *60*, 364−369.

(3) Maitra, U.; Bandyopadhyaya, A. K.; Sangeetha, N. M. *J. Org. Chem*. **2000**, *65*, 8239−8244.

(4) Davis, A. P.; Lawless, L. J. *Chem Commun*. **1999**, 9−10.

(5) D′Souza, L.; Maitra, U. *J. Org. Chem*. **1996**, *61*, 9494−9502.

(6) Takeuchi, T.; Chu, J.; Miwa, T. *Chromatographia* **1998**, *47*, 183−188.

(7) Vaton-Chanvrier, L.; Oulyadi, H.; Combret, Y.; Coquerel, G.; Combret, J. *Chirality* **2001**, *13*, 668−674.

(8) (a) Iuliano, A.; Salvadori, P.; Félix, G. *Tetrahedron*: *Asymmetry* **1999**, *10*, 3353−3364. (b) Iuliano, A.; Masini, G.; Salvadori, P.; Félix, G. *Tetrahedron*: *Asymmetry* **2001**, *12*, 2811−2825.

10.1021/jo0267450 CCC: $25.00
Published on Web 03/27/2003

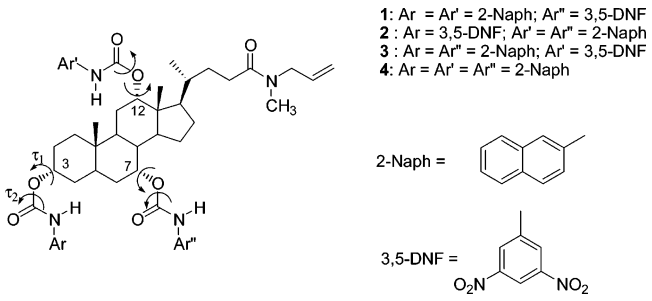

FIGURE 1. Chemical structures of compounds **1**−**4**.

because they were able to resolve not only derivatized racemic compounds but also some underivatized ones.[9] We have shown that the enantiodiscrimination capability of these CSPs depends on the electronic character of the aromatic moieties as well as on their arrangement on the cholestanic backbone.[9] To gain some insight into the origin of their peculiar stereodifferentiating capability, we examined, as a starting point, the conformational features of the cholestanic systems **1**−**4**.

Circular dichroism (CD) spectroscopy looks very suitable to this end because compounds **1**−**4** possess two chromophores, 2-naphthylcarbamate and 3,5-dinitrophenylcarbamate, having electrically allowed electronic transitions.[10] When electrically dipole allowed transitions are located in a chiral system, their oscillating dipoles can interact among themselves giving rise, in the CD spectrum, to a characteristic bisignate curve, named exciton couplet,[11] whose sign and intensity depend on the overall chemical structure of the compound and reflect its stereochemistry. This approach has thus been used for the nonempirical assignment of the absolute configuration to compounds with suitable chromophores in their structure[11] or after introducing them by derivatization of adequate functional groups already present in the molecule.[11] Since the absolute configuration of cholic acid is known, the presence of an exciton couplet can be used to determine the conformation of the compounds by comparing their experimental and calculated CD spectra: their agreement supports the molecular conformation used for the calculation as that preferentially assumed in solution. Therefore, to use CD spectroscopy for obtaining the molecular conformation, an adequate method to calculate the CD spectra is mandatory. The De Voe model[12] has proven to be effective for tackling this kind of problems.[13] According to this model, each allowed transition is represented in terms of experimental data, such as polarization direction and dipolar strength, in turn obtained from the ultraviolet (UV) spectra of suitable model compounds.[12] As starting geometries for carrying out these calculations, minimum energy conformations are required.

Since the molecules under scrutiny are made up of more than 135 atoms, we resorted to methods based on a force field definition that, unlike quantum mechanical (QM) calculations, do not have a near limit for the number of atoms. Furthermore, being parametrized on experimental data, they include dispersion contributions. Actually, attractive nonbonded interactions between aromatic rings are key constituents in determining the conformational stability of aromatic systems. Therefore dispersion interactions, which originate in induced dipole fluctuations, are essential to evaluate the interaction energies of aromatic side chains that, on the other hand, at the QM level depend crucially on the electron correlation procedure chosen and on the basis set employed.

To locate minimum energy structures on the conformational potential energy surface (PES), a variety of strategies have been developed. The most common approaches belong to two classes: deterministic methods and stochastic methods. Given the molecular complexity of compounds **1**−**4** the use of deterministic methods[14] results prohibitively expensive in terms of CPU time even for molecular mechanical force fields; therefore, stochastic methods were preferred.

Random search was thus used to investigate the conformational behavior of four cholic acid-based chiral selectors **1**−**4**, taking into account, in the rotatable bond selection, only the first two dihedrals of the side chains in positions 3, 7 and 12 on the central rigid backbone of the cholic acid ring system. All the initial structures were model-built with SYBYL,[15] while energy refinements were carried out with the Tripos force field and Gasteiger-Hückel charges.[16]

The aim of this work is to show how a combined approach using CD and molecular mechanics calculations allowed us to elucidate the stereochemical features of compounds **1**−**4**.

Results and Discussion

Random Search. Before presenting the structures associated to each spectrum, it is advisable to briefly describe the computational methods employed to derive them. The main purpose of a conformational analysis is to locate the global minimum on the PES. It must be taken into account, however, that although the global minimum corresponds to the most stable conformation, it may not be highly populated, because of peculiar features of the PES. In addition, a molecule can adopt more than a single stable conformation. The presence of the environment as well may affect a compound three-dimensional structure, shifting the equilibrium from a conformer to another. This is the reason why a number of low energy conformers are usually considered. Moreover, when a few energy minima have been located within a specific potential energy function, their relative energy

(9) Iuliano, A.; Pieraccini, I.; Salvadori, P.; Félix, G. *Tetrahedron*: *Asymmetry* **2002**, *13*, 1265−1275.

(10) Jaffé, A.; Orchin, M. *Theory and Application of UV Spectroscopy*; Wiley: New York, 1962.

(11) (a) Harada, N.; Nakanishi, K. *Circular Dichroic Spectroscopy, Exciton coupling in Organic Stereochemistry*; University Science Books: Oxford, 1983. (b) Lightner, D.; Gurst, J. E. *Organic Conformational Analysis and Stereochemistry from Circular Dichroism Spectroscopy*; Wiley-VCH: New York, 2000.

(12) (a) De Voe, H. *J. Chem. Phys.* **1964**, *41*, 393−400. (b) DeVoe, H. *J. Chem. Phys.* **1965**, *43*, 3199−3208. (c) Rosini, C.; Zandomeneghi, M.; Salvadori, P. *Tetrahedron*: *Asymmetry* **1993**, *4*, 545−554.

(13) (a) Iuliano, A.; Franchi, E.; Uccello-Barretta, G.; Salvadori, P. *J. Org. Chem.* **1998**, *63*, 8765−8768. (b) Iuliano, A.; Voir, I.; Salvadori, P. *Eur. J. Org. Chem.* **2000**, 1767−1772.

(14) For a molecule with six rotatable bonds, such as compounds **1**−**4**, even considering a dihedral angle increment of 60°, 46 656 conformations need to be calculated.

(15) SYBYL Molecular Modelling Software, Version 6.7, TRIPOS Associates, St. Louis, MO, October 2000.

(16) (a) Gasteiger, J.; Marsili, M. *Tetrahedron* **1980**, *36*, 3219−3228. (b) Gasteiger, J.; Saller, H. *Angew. Chem., Int. Ed. Engl.* **1985**, *24*, 687−689. (c) Hückel, E. *Z. Phys.* **1932**, *76*, 628.

values are unlikely conserved using a different force field and, in some cases, it is difficult to establish the reliability of the description.

To cross-check structures and energies, the four compounds have been studied using two different force fields: Tripos, coupled with Gasteiger−Hückel charges, and the Merck Molecular Force Field (MMFF94).[17] Tripos was developed for handling a broad range of organic and bioorganic molecules, but it is not particularly concerned about reproducing some of the subtleties of molecular structure. Satisfactory results as compared to high level ab initio calculations were anyway obtained for aromatic systems.[18,19] MMFF94, whose functional form resembles MM2[20] and MM3[21] as well as MM2X,[22] was parametrized for an unusually wide variety of chemical systems and its charge assignment protocol makes use of additive bond charge increments (BCI), associating a parameter to each class of bonds. The BCI parameters, similar in physical motivation to the bond dipoles used in MM2 and MM3, give results almost identical with MM2 and MM3.

The X-ray resolved structure of cholic acid contained in the Cambridge Structural Database (CSD)[23] was chosen as a starting point in the construction process (CSD code: CHOLET01).[24] 2-Naphthylcarbamate and 3,5-dinitrophenylcarbamate groups were attached to the hydroxyl groups in order to obtain the four compounds under investigation, and their starting structures were energy minimized.

Random torsion searching was performed for each molecule starting from different initial conformations reducing the total number of rotatable bonds to six (Figure 1). Since we are interested in the mutual position of the C-3, C-7, and C-12 substituents, the dihedral angles defining the orientation of the C-17 side chain, which does not contribute to the compound UV and CD spectra, were not scanned. It was assumed that their conformations were refined during the minimization process.

Carbamate groups can exist as syn or anti rotamers with the anti rotamer favored by 1.0−1.5 kcal mol^{-1} for steric and electrostatic reasons.[25] Nudelman and coworkers[25] reported that, at low temperature, the syn/anti rotamer ratio for *N*-alkylcarbamates in $CDCl_3$ solution is ∼0.1, whereas for *N*-aromatic carbamate the ratio is ∼0.05, thus indicating that syn rotamers are particularly disfavored. From experimental data, the barrier for rotation about an *N*-alkylcarbamate C(carbonyl)−N bond is usually around 16 kcal mol^{-1},[26] while the rotation barrier is even lower (12.5 kcal mol^{-1}) in the case of an *N*-phenylcarbamate.

A model system, methylphenylcarbamate, was optimized ab initio at the SCF/6-31G* level considering either the syn or anti conformer. The final structures showed a coplanar arrangement of the carbamate group with respect to the benzene ring with a small energy difference between syn and anti conformations (∼2.4 kcal mol^{-1}) favoring the anti arrangement. Anti conformations were thus chosen for the carbamate groups of the compounds under scrutiny, further reducing the number of degrees of freedom to explore during the random search. Nonetheless, torsional angles not considered as rotatable bonds were allowed to relax during the minimization phase. Conversely, chirality was forced to remain constant.

All conformational searches were run without explicit solvent molecules, but applying a dielectric constant of 37, corresponding to acetonitrile, the solvent employed in the experimental work, to damp electrostatic interactions and simulate the solvent screening effect. The conformers were accepted when their energy gap was within 20 kcal mol^{-1} of the lowest energy conformer and the root-mean-square (rms) deviation, obtained by superimposing the heavy atoms of the new conformation with those of the already accepted conformations, was greater than 0.2 Å to avoid multiple copies. A total number of ∼1000 conformers for each compound was considered and analyzed. The energy threshold chosen can appear large, but experimental results may be affected by high-energy conformers evoking a stronger CD response.

Due to the possible limitations of the force fields and to the lack of environmental effects, which are, however, expected to be small in non hydrogen-bonded systems, we preferred to examine a wealth of structures to prevent discarding significant conformers. Despite these warnings, in fact, it is reasonable to suppose that, among the conformations found, there are the relatively low energy structures responsible for the observed spectral properties that produce the characteristic CD bands.

Structural Analysis. We report the conformer populations generated for each compound in the form of histograms. The results obtained with MMFF94 are consistent with those obtained using the Tripos force field. Thus, only the latter results are shown.

Ring Distances. The separations of the ring centroids are plotted versus the density (fraction of the sum of counts divided by the bin width) of low energy conformers ($\Delta E \leq 10$ kcal mol^{-1}) that exhibit the given distance in each 1 Å interval in the histograms shown in Figure 2. To simplify the notation, the centroids of the rings in the C-3, C-7, and C-12 positions are named X3, X7, and X12, respectively. In Figure 2, the molecules are ordered so as to gather the naphthalene ring centroid distance histograms (**a**, **e**, **i**) along the major diagonal of the graph matrix.

(17) (a) Halgren, T. A. *J. Comput. Chem.* **1996**, *17*, 490−519. (b) Halgren, T. A. *J. Comput. Chem.* **1996**, *17*, 520−552. (c) Halgren, T. A. *J. Comput. Chem.* **1996**, *17*, 553−586. (d) Halgren, T. A.; Nachbar, R. B. *J. Comput. Chem.* **1996**, *17*, 587−615. (e) Halgren, T. A. *J. Comput. Chem.* **1996**, *17*, 616−641.

(18) Alagona, G.; Ghio, C.; Giolitti, A.; Monti, S. *Theor. Chem. Acc.* **1999**, *101*, 143−150.

(19) Alagona, G.; Ghio, C.; Monti, S. *Int. J. Quantum Chem.* **2002**, *88*, 133−146.

(20) Allinger, N. L. *J. Am. Chem. Soc.* **1977**, *89*, 8127−8134.

(21) Allinger, N. L.; Yuh, Y. H.; Lii, J. H. *J. Am. Chem. Soc.* **1989**, *111*, 8551−8566.

(22) Holloway, M. K.; Wai, J. M.; Halgren, T. A.; Fitzgerald, D. P. M.; Vacca, J. P.; Dorsey, B. D.; Levin, R. B.; Thompson, W. J.; Chen, L. J.; deSolms, S. J.; Gaffin, N.; Ghosh, A. K.; Giuliani, E. A.; Graham, S. L.; Guare, J. P.; Hungate, R. W.; Lyle, T. A.; Sanders, W. M.; Tucker, T. J.; Wiggins, M.; Wiscount, C. M.; Woltersdorf, O. W.; Young, S. D.; Darke, P. L.; Zungay, J. A. *J. Med. Chem.* **1995**, *38*, 305−308.

(23) Allen, F. H.; Bellard, S.; Brice, M. D.; Cartwright-Doudleday, B. A.; Higgs, H.; Hummelink, T.; Hummelink-Peters, B. G.; Motherwell, W. D. S.; Rodgers, J. R.; Watson, D. G. *Acta Crystallogr. Sect. B* **1979**, *53*, 2331−2339.

(24) Jones, E. L.; Nassimbeni, L. R. *Acta Crystallogr. Sect. B (Str. Sci.)* **1990**, *46*, 399−405.

(25) Marcovici-Mizrahi, D.; Gottlieb, H. E.; Marks, V.; Nudelman, A. *J. Org. Chem.* **1996**, *61*, 8402−8406.

(26) (a) Rablen, P. R. *J. Org. Chem.* **2000**, *65*, 7930−7937. (b) Lectka, T.; Cox, C. *J. Org. Chem.* **1998**, *63*, 2426−2427. (c) Kost, D.; Kornberg, N. *Tetrahedron Lett.* **1978**, *35*, 3275−3276.

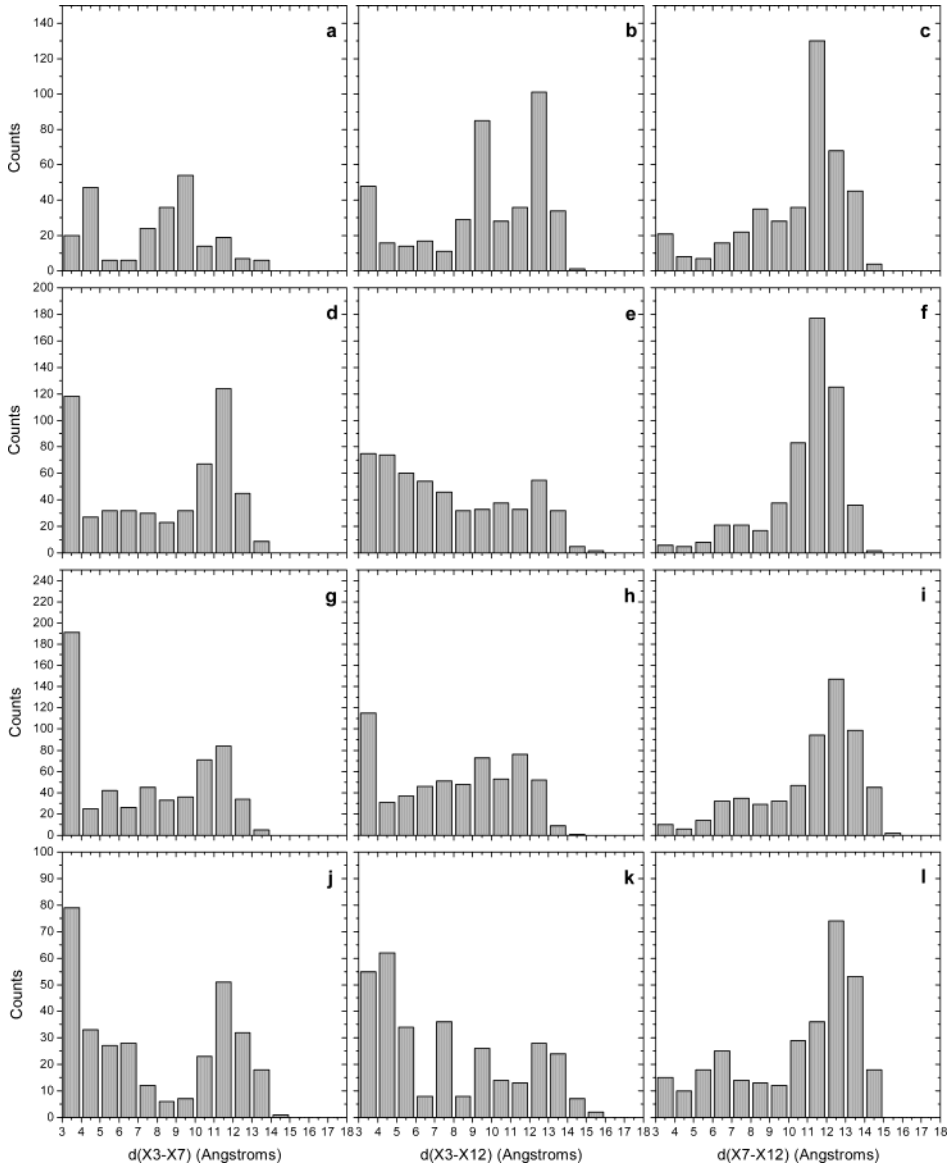

FIGURE 2. Number of low energy ($\Delta E \leq 10$ kcal mol^{-1}) conformers for each indicated distance between the ring centroids (X3−X7, X3−X12, and X7−X12) produced by the random search protocol for molecule **3** (top line), molecule **1** (second line), molecule **2** (third line), and molecule **4** (bottom line).

The distribution shapes for the naphthyl ring centroid distances of molecules **3** and **1**, **a** and **e**, are bimodal with peaks in the 4−5, 9−10 Å and 3−5, 12−13 Å intervals, respectively, indicating two possibilities: conformations in which the two ring systems are stacked and can weakly interact with each other (4−5 and 3−5 Å) and conformations in which these two side-chains are far apart (9−10 and 12−13 Å); whereas for molecule **2**, **i**, the most common low energy conformers have only a large centroid separation, i.e., in the 12−13 Å range.

As far as the dinitrophenyl position is concerned, for molecule **3** the X3−X12 distance distribution, **b**, has a maximum in the range 12−13 Å, a significant number of structures in the range 9−10 Å, and a lower number of conformations in the range 3−4 Å. The X7−X12 distance distribution, **c**, has a maximum in the range 11−12 Å, but all the other distances are less populated. In the corresponding conformations, the dinitrophenyl ring is either far from both naphthyl rings or far from the C-7 naphthyl ring and stacked with the naphthyl ring in C-3 position. For molecule **1**, the dinitrophenyl−naphthyl centroid separation, **d** and **f**, in most conformers is in the 11−12 Å range, but conformations with dinitrophenyl stacking with the C-3 naphthyl ring are also present (**d**). In the case of molecule **2** the situation is different: the most common distance between the dinitro centroid and both naphthyl centroids, **g** and **h**, is in the range 3−4 Å suggesting that dinitrophenyl can be involved in stacking interactions with one ring or the other or both of them, but with a marked preference for the naphthyl in the C-3 position (**g**). In the case of molecule **4**, the distributions of the X3−X7 and X7−X12 centroid distances, **j** and **l**, are bimodal with peaks in the 3−4, 11−12 Å and 6−7, 12−13 Å intervals, respectively, whereas the distribution of X3−X12 centroid separations, **k**, is more scattered.

Torsional Angles. The distributions of individual and multiple dihedral angles $\tau_1(3)$, $\tau_2(3)$, $\tau_1(7)$, $\tau_2(7)$, $\tau_1(12)$, $\tau_2(12)$ (indicated by arrows in Figure 1) may provide a

useful insight into the conformational properties of these molecules and describe the shape of the side chains. The exact numerical values of the dihedral angles were converted to the common symbolic terms cis (**C**: dihedrals falling in the sector −30° to +30°), gauche (**G**$^+$: dihedrals falling in the sector 30° to 90°; **G**$^-$: dihedrals falling in the sector −90° to −30°), anticlinal (**A**$^+$: dihedrals falling in the sector 90° to 150°; **A**$^-$: dihedral falling in the sector −150° to −90°) and trans (**T**: dihedrals falling in the sector −150° to +150°).

The most stable conformations for each molecule, i.e., those within 5 kcal mol^{-1} (case **L**) and then within 10 kcal mol^{-1} (case **H**) of the lowest energy conformer, were analyzed.

Molecule 1. Individual distributions of $\tau_1(3)$ and $\tau_2(3)$ showed peaks in the **T**, **G**$^+$ and **G**$^-$ regions and in the **T** region, respectively; these dihedral angles were arranged as (**T**,**T**) or (**G**$^+$,**T**) pairs in case **L,** but in case **H** a new pair (**G**$^-$,**T**) appeared. On the contrary, $\tau_1(7)$ and $\tau_2(7)$ individual distributions showed peaks in the **G**$^-$ and **T** region, respectively, and were arranged as (**G**$^-$,**T**) pairs. $\tau_1(12)$ and $\tau_2(12)$ individual distributions showed marked peaks in the **T** and **A**$^+$ regions, respectively, and they were arranged as (**T**,**A**$^+$) or (**T**,**T**) pairs with a prevalence for (**T**,**A**$^+$) pairs.

Molecule 2. The dihedral angle distributions obtained for this molecule presented a wide spreading over a large area when higher energy differences were considered (case **H**). Similarly to molecule **1**, individual distributions of $\tau_1(3)$ and $\tau_2(3)$ showed marked peaks in the **T**, **G**$^+$ and **G**$^-$ regions and in the **T** region, respectively, although the (**T**,**T**) and (**G**$^+$,**T**) pairs remained the most populated, in case **L,** while the contribution of (**G**$^-$,**T**) conformers, in case **H**, was quite appreciable. The most common $\tau_1(7)$ and $\tau_2(7)$ values, in case **L**, were in the **G**$^-$ and **T** region, respectively, but in case **H** equally populated conformations with **G**$^+$ and **C** peaks for $\tau_2(7)$ were found. However, $\tau_1(7)$ and $\tau_2(7)$ were arranged mostly as (**G**$^-$,**T**) pairs. Both $\tau_1(12)$ and $\tau_2(12)$ individual distributions showed peaks in the **T** region and were consequently arranged as (**T**,**T**) pairs.

Molecule 3. $\tau_1(3)$ and $\tau_2(3)$ most populated values were in the **T** region; thus, they were arranged mostly as (**T**,**T**) pairs. However (**G**$^+$,**T**) pairs were also considerably populated. Both $\tau_1(7)$ and $\tau_2(7)$ individual distributions showed peaks in the **T** region in case **L**, whereas in case **H** the most populated values for $\tau_1(7)$ were in the **G**$^-$ region. These angles were arranged mostly as (**G**$^-$,**T**) pairs. Conversely, the most common $\tau_1(12)$ and $\tau_2(12)$ angles were in the **T** region and they were arranged as (**T**,**T**) pairs.

Molecule 4. As before, the six dihedral angles examined had the same qualitative distributions. Their inspection indicated that the most stable conformations of the molecules under study were those in which the bonds C−O, O−C in C-3 position adopted the (**T**,**T**), (**G**$^+$,**T**), or (**G**$^-$,**T**) conformations, with the (**G**$^-$,**T**) and (**T**,**T**) forms prevailing for bonds in C-7 and C-12 positions, respectively. This preference was weakened for molecule **1** that could assume a (**T**,**A**$^+$) form as well.

Analysis of the CD Spectra of Compounds 1−4. As stated above, the cholic acid derivatives **1**−**4** possess two chromophores, 2-naphthylcarbamate and 3,5-dinitrophenylcarbamate. The UV spectrum (see Figure S1 in the Supporting Information) of *N*-allyl-*N*′-methyl-3-(2-naphthyl)carbamoyloxy-7,12-dihydroxycholan-24-amide, chosen as a model compound for the naphthylcarbamate chromophore, shows an absorption band at 280 nm (ϵ = 8300), endowed with vibrational structure, attributable to an electrically allowed transition polarized along the short axis of the naphthalene ring and a strong band having two maxima, the former at 240 nm (ϵ = 75 000) and the latter at 235 nm (ϵ = 68 000), attributable to two electrically allowed transitions polarized along the long axis of the aromatic group and along the C2−C7 axis of the naphthalene ring, respectively. The assignment of these bands has been made on the basis of the high similarity between this spectrum and the UV spectrum of 2-naphthylamine whose transitions are well-known.[27] Only a weak positive Cotton effect is present in the CD spectrum (also displayed in Figure S1) at 240 nm ($\Delta\epsilon$ = 5), due to the asymmetrically perturbed transitions of the 2-naphthylcarbamate chromophore.

The UV spectrum of **1** (Figure 3a) shows an absorption region centered at 280 nm, endowed with vibrational structure (ϵ = 17 000), attributable to the transition polarized along the short axis of the 2-naphthylcarbamate chromophores and an intense band endowed with two maxima at 242 and 238 nm (ϵ = 160 000) attributable to the electrically dipole allowed transitions of the 2-naphthylcarbamate chromophores.

This spectrum is very similar, as far as number, position and shape of the bands are concerned, to the UV spectrum of the model compound. The sole difference is the intensity of the bands that is doubled, since this derivative possesses a pair of 2-naphthylcarbamate instead of one as the model compound. The presence of 3,5-dinitrophenylcarbamate seemingly does not have an appreciable influence on the UV spectrum of **1**. This is not surprising because the 3,5-dinitrophenylcarbamate chromophore[28] possesses two absorption bands, at 255 nm (ϵ = 10 700) and at 225 nm (ϵ = 22 500), which are buried by the stronger absorption bands of the pair of 2-naphthylcarbamate chromophores. The CD spectrum (Figure 3a) shows a feeble, positive Cotton effect centered at 280 nm ($\Delta\epsilon$ = +5) and two more intense bands, having opposite sign, at 245 nm ($\Delta\epsilon$ = +100) and at 230 nm ($\Delta\epsilon$ = −40). These two Cotton effects are likely the components of an exciton couplet centered at 235 nm, having an amplitude[11] of 140, due to the coupling of the electrically dipole allowed transitions of the pair of 2-naphthylcarbamate chromophores.[29]

The presence of an exciton couplet in the CD spectrum suggests that the involved transitions have to assume a statistically definite mutual orientation:[11] therefore, from the CD spectrum of **1** a reduced conformational freedom of the 2-naphthylcarbamate groups can be inferred. It is worth noting that the presence of the 3,5-dinitrophenylcarbamate moiety gives a negligible contribution to the CD absorption of **1**, as can be deduced by comparing the

(27) Tanizaki, Y.; Kobayashi, M. *Spectrochim. Acta* **1972**, *28A*, 2351−2366.

(28) The UV spectrum was recorded on the ethyl 3,5-dinitrophenylcarbamate, used as a model compound.

(29) The exciton couplet is scarcely symmetric (the two Cotton effects have different intensity); anyway, the increased intensity of the CD bands of **1** with respect to those of the model compounds,[11] confirms that the succession of the two oppositely signed Cotton effects constitutes an exciton couplet.

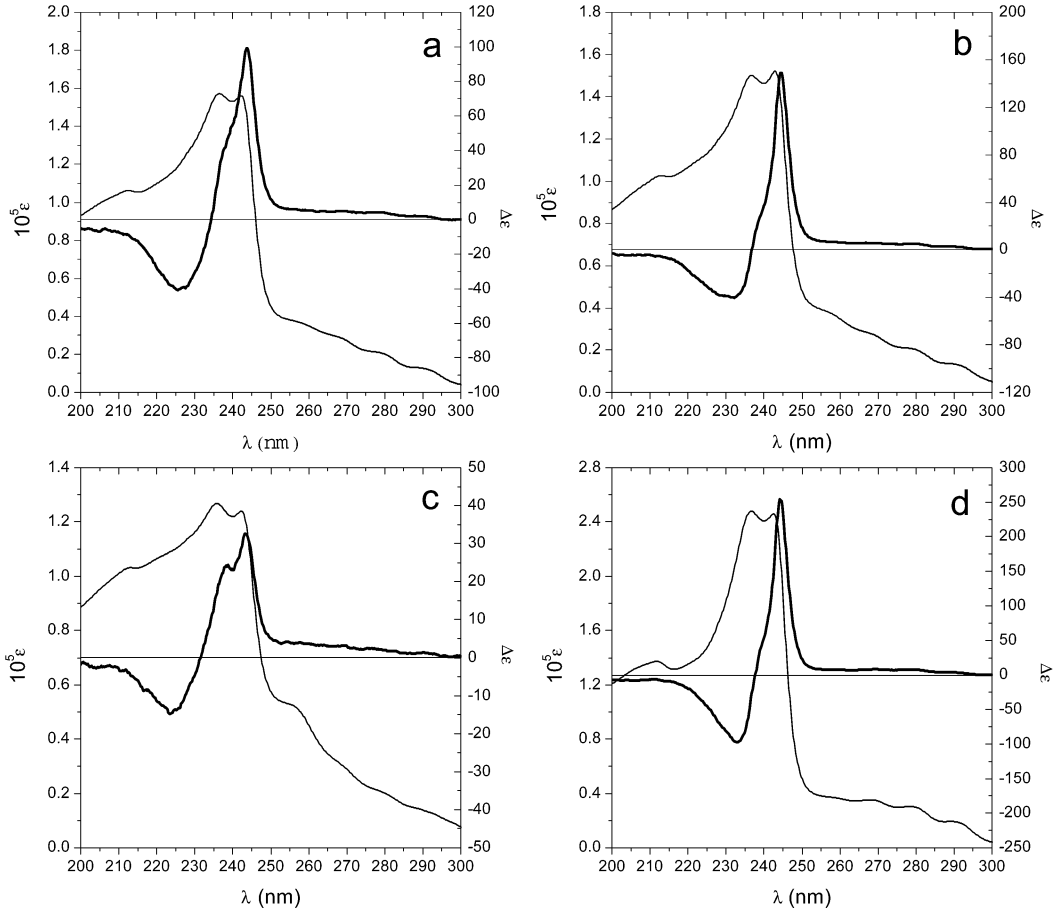

FIGURE 3. Experimental UV (thin line) and CD (bold line) spectra of compounds **1** (a), **2** (b), **3** (c), **4** (d); ϵ and $\Delta\epsilon$ in mol^{-1} cm^{-1}.

CD spectrum of **1** (Figure 3a) with the CD spectrum of the corresponding 3,12-dinaphthylcarbamoyl derivative of cholic acid (see Figure S2, Supporting Information) devoid of the 3,5-dinitrophenylcarbamate group at position 7. The lack of coupling between the transitions of the 3,5-dinitrophenylcarbamate group and the transitions of the 2-naphthylcarbamate moieties is also deduced from the analysis of the CD spectrum of a cholic acid derivative bearing a 2-naphthylcarbamate group at position 3 and a 3,5-dinitrophenylcarbamate moiety at position 12 (see Figure S3, Supporting Information): not only does this CD spectrum not show the presence of any exciton couplet, but also it is substantially superimposable to the CD spectrum of the cholic acid derivative bearing only the 2-naphthylcarbamate group at position 3 (Figure S1, Supporting Information).

The UV spectrum of **2** (Figure 3b) is very similar to the UV spectrum of **1**, as far as number, shape, position, and intensity of the absorption bands are concerned: an absorption band centered at 280 nm together with two absorption maxima at 242 and 237 nm ($\epsilon = 155\,000$) are present. Also in this case the presence of a 3,5-dinitrophenylcarbamate group has no influence on the UV spectrum, which is dominated by the electronic transitions of the 2-naphthylcarbamate chromophores. An exciton couplet centered at 235 nm is present also in the CD spectrum of **2** (Figure 3b); therefore, the 2-naphthylcarbamate chromophores interact with each other also when these groups are located at positions 7 and 12 of the cholestanic system. The amplitude ($A = 190$) of the couplet is higher than in the CD spectrum of **1**. The amplitude of the split type Cotton effects in systems whose chromophores are exciton coupled depends on the angle between the transition dipole moment vectors of the two coupled chromophores as well as on their distance.[11] In this case, both phenomena can contribute to increasing the intensity of the couplet. In fact, positions 7 and 12 of the cholestanic system are closer[23] than positions 3 and 12. In addition, due to the different mutual arrangement of the pair of 2-naphthylcarbamate groups, the angle between their transition dipole moments can be different with respect to the previous case.

The dependence of the amplitude of the exciton couplet on the different disposition of the substituent on the cholestanic backbone is confirmed by the analysis of the CD spectrum of **3** (Figure 3c), which possesses a pair of 2-naphthylcarbamate groups at positions 3 and 7 of the steroidal skeleton. This spectrum still shows an exciton couplet centered at 235 nm, whose lower amplitude ($A = 49$) can be attributed to the larger separation[26] between positions 3 and 7 of the cholestanic backbone as well as to a different angle between the transition dipole moments of the interacting chromophores. The low energy component of the exciton couplet shows a shoulder at about 240 nm probably due to the greater influence that the presence of a 3,5-dinitrophenylcarbamate chromophore exerts on the dichroic absorption of **3**. This influence can be invoked also to explain the lower intensity of the UV absorption band at 240 nm ($\epsilon = 130\,000$).

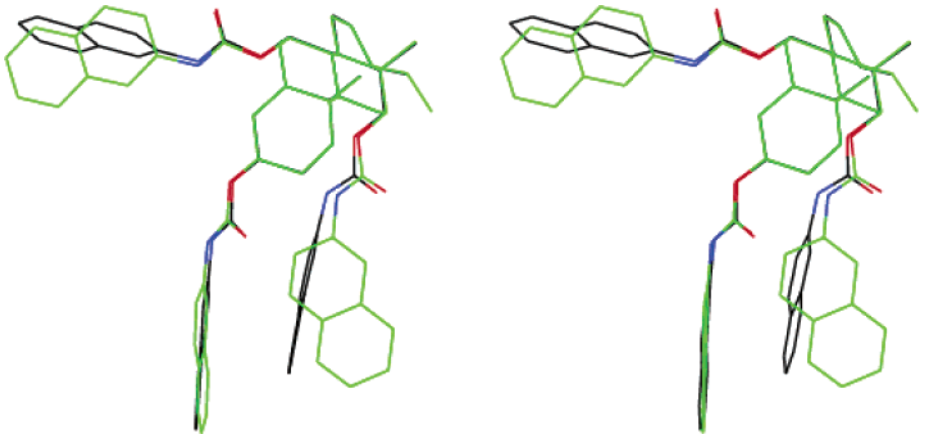

FIGURE 4. Stereoview of two minimum energy conformations, superimposed on the cholestanic backbone atoms, of compound **4** whose theoretical CD spectra agreed acceptably well with the experimental one: for the sake of clarity, hydrogen atoms and the alkyl chain at 17-position are not displayed.

The UV spectrum (Figure 3d) of **4** looks very similar to the UV spectra of the other derivatives as far as number, position and shape of the absorption bands are concerned. It shows an absorption band centered at 280 nm (ϵ = 27 000), endowed with vibrational structure, attributable to the transition polarized along the short axis of the 2-naphthylcarbamate chromophores, and a more intense band having two maxima at 242 and 238 nm (ϵ = 250 000) attributable to the electrically dipole allowed transitions polarized along the long axis of the 2-naphthylcarbamate groups. The intensity of the bands is three times as much as the intensity of the corresponding bands of the model compound: this is obvious because of the presence of three 2-naphthylcarbamate groups in derivative **4**. The CD spectrum (Figure 3d) shows an exciton couplet centered at 240 nm attributable to the coupling of the electrically allowed transition of the three 2-naphthylcarbamate chromophores located at positions 3, 7, and 12 of the cholestanic system. The amplitude of the exciton couplet present in the CD spectrum of **4** has a value (A = 351) corresponding to the sum of the amplitudes of the exciton couplets of the CD spectra of **1**, **2**, and **3**. Such additivity suggests that the mutual disposition of each couple of 2-naphthylcarbamate groups of **4** (3−12, 12−7, 7−3) is very similar to that assumed by the same pair in derivatives **1**, **2**, and **3**. In fact, since the amplitude of an exciton couplet depends on the angle between the dipole moments of the interacting chromophores,[11] the additivity indicates that the dihedral angle between each couple of chromophores in **4** is close to the value taken in the corresponding bis-2-naphthylcarbamate derivative.[13] In other words, this means that the pair of 2-naphthylcarbamate groups located at positions 3 and 12 of the cholestanic backbone of **4** assumes a similar disposition as in **1**, the pair of 2-naphthylcarbamate groups at positions 12 and 7 of **4** are mutually arranged as in **2** and the pair of 2-naphthylcarbamate groups at positions 7 and 3 of **4** are mutually oriented as in **3**.

Conformer Selection: The De Voe Approach

To further limit the number of analyzed conformers, theoretical CD spectra, obtained using a calculation method based on the De Voe coupled oscillator theory,[12] were compared to the experimental ones. This approach was successfully employed to assess the favored conformations of poly(iminomethylenes).[30] To perform these calculations, the allowed transitions of each chromophore were described in terms of a single dipole located in the center of the chromophore, having a dipolar strength calculated from the experimental UV spectra of the model compounds and direction determined via semiempirical calculations. The semiempirical computational approach consisted in the generation of excitation spectra, using the ZINDO module of the MSI Cerius^2 software,[31] of the isolated chromophores, i.e., β-naphthylamine and 3,5-dinitrophenylcarbamate, whose geometries were obtained using SYBYL.

As a first step, we calculated the CD spectra of **4**, using the minimum energy conformations obtained according to the aforementioned procedure. To perform these calculations, the transitions in the spectral range 235−240 nm were described by means of a single dipole located in the center of the naphthalene system and directed along its C2−C7 axis; a dipolar strength of 55 D^2 centered at 238 nm was attributed to it to satisfactorily reproduce the UV absorption band. Each calculated CD spectrum was compared to the experimental one. Among the minimum energy structures whose theoretical CD spectra agreed acceptably well with the experimental ones (as far as sign, number, position, and order of magnitude of the dichroic bands are concerned), we decided to choose as representative conformations those whose $\tau_{1,2}(3)$, $\tau_{1,2}(7)$, and $\tau_{1,2}(12)$ torsional angles were arranged as (**G**$^-$,**T**), (**G**$^-$,**T**), and (**T**,**T**) pairs, respectively, that were among the most populated ones. Two possible geometries of **4** (i.e., **4a** and **4b**) superimposed on the carbon atoms of the cholestanic backbone are shown in Figure 4 (their theoretical spectra are reported later in Figure 7d as compared to the experimental one).

They have X3−X7 centroid distances of 11 and 12 Å, respectively; their naphthyl rings have a different spatial disposition, but the dipole moments chosen for the De Voe calculations have a similar mutual orientation with a maximum angular difference of about 10°, as can be

(30) Clericuzio, M.; Alagona, G.; Ghio, C.; Salvadori, P. *J. Am. Chem. Soc.* **1997**, *119*, 1059−1071.
(31) MSI Cerius^2, version 4.2, Molecular Simulation Inc., San Diego, CA, **2000**.

TABLE 1. Ring Centroid Distances (Å) and Angles between the Naphthalene Ring Dipoles (deg) of Selected Conformations

	distances[a]			angles		
molecule	X3−X7	X3−X12	X7−X12	D3−D7	D3−D12	D7−D12
4a	***11***	***6***	***12***	88	16	96
4b	***12***	***5***	***12***	99	12	96
3	***12***	12	12	104		
1	11	***6***	10		11	
2	10	8	***12***			96

[a] The naphthalene ring centroid distances are reported in bold italic.

seen from Table 1, where the ring centroid distances and angles between the naphthalene ring dipoles are reported for those structures.

To obtain the calculated CD spectra of compounds **1**−**3**, in addition to the oscillators describing the transitions of two 2-naphthylcarbamate chromophores, the transitions of the 3,5-dinitrophenyl carbamate chromophore were considered. These transitions were described by means of two dipoles located in the center of the 3,5-dinitrophenylcarbamate chromophore, the first one centered at 225 nm and polarized along the axis joining the two nitro group nitrogens, the second one centered at 255 nm and polarized along a direction perpendicular to the previous one. Dipolar strengths of 15 and 7.5 D^2, respectively, were attributed to them in order to satisfactorily reproduce the UV absorption bands. Minimum energy conformations differing for the aromatic rings spatial disposition showed similar theoretical CD spectra consistent with the experimental ones (as far as sign, number, position, and order of magnitude of the dichroic bands are concerned).

To further evaluate the agreement between experimental and theoretical CD spectra, the parameters characterizing the positive peak of the exciton couplet, i.e., wavelength (λ), height (H), width (W), area (A), and the wavelength within the couplet where $\Delta\epsilon$ is 0 (λ_0) have been taken into account. The similarity percentages (S%) of each parameter p, defined as $100 \times (p_{Th} - p_{Exp})/p_{Exp}$, are reported in Table 2 together with rough assignments of $\tau_{1,2}(3)$, $\tau_{1,2}(7)$, and $\tau_{1,2}(12)$ torsional angles and ring centroid distances X3−X7, X3−X12, X7−X12 (for more details see Table S4, Supporting Information).

A number of calculated CD spectra are reported in Figure 5. For molecule **1**, two curves (1e and 1g), discarded according to qualitative criteria, are also shown for comparison. The spectra of both structures display more CD bands than the experimental ones: structure 1g shows also a negative band at about 256 nm ($\Delta\epsilon = -28$), while structure 1e shows two negative bands, one at 224 nm ($\Delta\epsilon = -195$) and the other at 234 nm ($\Delta\epsilon = -68$), instead of just one.

The structures with minimum numbers of acceptable S% have been discarded, while the remaining ones, i.e., structures 1a, 1c, 1d, 1f, 2a, 2b, 2c, 2d, 2e, 2f, and 3a, 3c, 3d were further analyzed.

Among the structures retained after the previous screenings, we looked for those whose torsional angles were among the most populated ones and with the two 2-naphthylcarbamate groups arranged in a similar spatial position as in compound **4**. On the basis of these additional criteria, a reduced number of molecular conformations, shown in Figure 6, have been identified, whose spectra are displayed in Figure 7. As can be seen from Table 2 and Figure S6 (Supporting Information), the selection for compound **2** is difficult, since each of the examined conformations can be a good candidate: the mutual disposition of the 2-naphthylcarbamate groups, in fact, indicates that the selected molecules can be considered as members of the same family.

In Figures S5−S8 (Supporting Information) comparisons between the chosen conformations and the structures discarded during the final selection superimposed

TABLE 2. Similarity Percentages between Area, Wavelength, Width, Height, $\Delta\epsilon = 0$ Wavelength of Theoretical and Experimental Bands for a Number of Conformers of Molecules 1−4, Described by the Dihedral Angles for Each Substituent and by the Separation between Each Couple of Substituent Centroids[a]

molecule	S%A	S%λ	S%W	S%H	S%λ_0	$\tau_{1,2}(3)$	$\tau_{1,2}(7)$	$\tau_{1,2}(12)$	X3−X7	X3−X12	X7−X12
1a	**20.6**	**0.9**	**28.9**	**0.3**	**1.6**	**(G^-,T)**	**(G^-,T)**	**(T,A^+)**	**11**	**5**	**10**
1b	67.7	1.4	28.9	39.7	0.9	(T,T)	(G^-,T)	(T,T)	4	13	12
1c	12.6	0.9	27.8	6.1	1.7	(G^-,T)	(G^-,T)	(T,A^+)	11	11	12
1d	19.1	1.9	2.2	21.1	1.0	(T,T)	(G^-,T)	(T,A^+)	4	13	12
1f	24.4	0.1	0.0	20.8	1.5	(G^-,T)	(G^-,T)	(T,A^+)	11	6	10
2a	**79.9**	**1.1**	**26.7**	**9.5**	**0.2**	**(G^-,T)**	**(G^-,T)**	**(T,T)**	**10**	**7**	**12**
2b	73.7	1.4	26.7	4.2	0.2	(T,T)	(G^-,T)	(T,T)	6	10	13
2c	44.4	1.1	26.7	11.9	0.2	(G^-,T)	(G^-,T)	(T,T)	9	7	11
2d	38.2	1.4	26.7	18.4	0.1	(G^-,T)	(G^-,T)	(T,T)	11	10	12
2e	71.1	1.4	3.3	3.8	0.2	(T,T)	(G^-,T)	(T,T)	6	11	13
2f	38.3	1.1	26.7	16.6	0.1	(G^+,T)	(G^-,T)	(T,T)	8	6	13
2g	64.1	1.4	36.7	4.3	0.3	(G^-,T)	(G^-,T)	(T,T)	10	8	12
3a	**61.2**	**0.9**	**20.8**	**39.6**	**2.3**	**(G^-,T)**	**(G^-,T)**	**(T,T)**	**12**	**12**	**12**
3b	102.5	0.7	27.1	90.5	2.8	(G^-,T)	(G^-,C)	(T,C)	13	15	10
3c	15.7	0.7	20.8	8.0	2.9	(G^-,T)	(G^-,C)	(G^+,T)	13	14	12
3d	67.8	0.5	12.5	12.0	1.6	(T,T)	(G^-,T)	(T,T)	5	12	12
3e	70.7	0.9	33.3	53.1	2.3	(G^-,T)	(A^-,T)	(A^-,G^-)	13	10	13
4a	**97.0**	**0.4**	**25.8**	**4.1**	**0.8**	**(G^-,T)**	**(G^-,T)**	**(T,T)**	**11**	**6**	**12**
4b	**65.3**	**0.6**	**4.8**	**3.8**	**0.4**	**(G^-,T)**	**(G^-,T)**	**(T,T)**	**12**	**5**	**12**
4c	68.2	0.6	33.9	13.3	0.0	(G^-,T)	(T,A^-)	(T,T)	12	10	5
4d	61.7	1.1	22.6	4.8	0.1	(T,T)	(A^-,A^-)	(T,T)	11	12	9
4e	48.4	0.6	4.8	17.2	0.3	(G^-,T)	(G^-,T)	(A^+,A^-)	8	7	5
4f	64.0	0.4	4.8	9.1	0.4	(G^-,T)	(A^-,A^-)	(T,T)	12	5	9

[a] The boldface values refer to the selected structures.

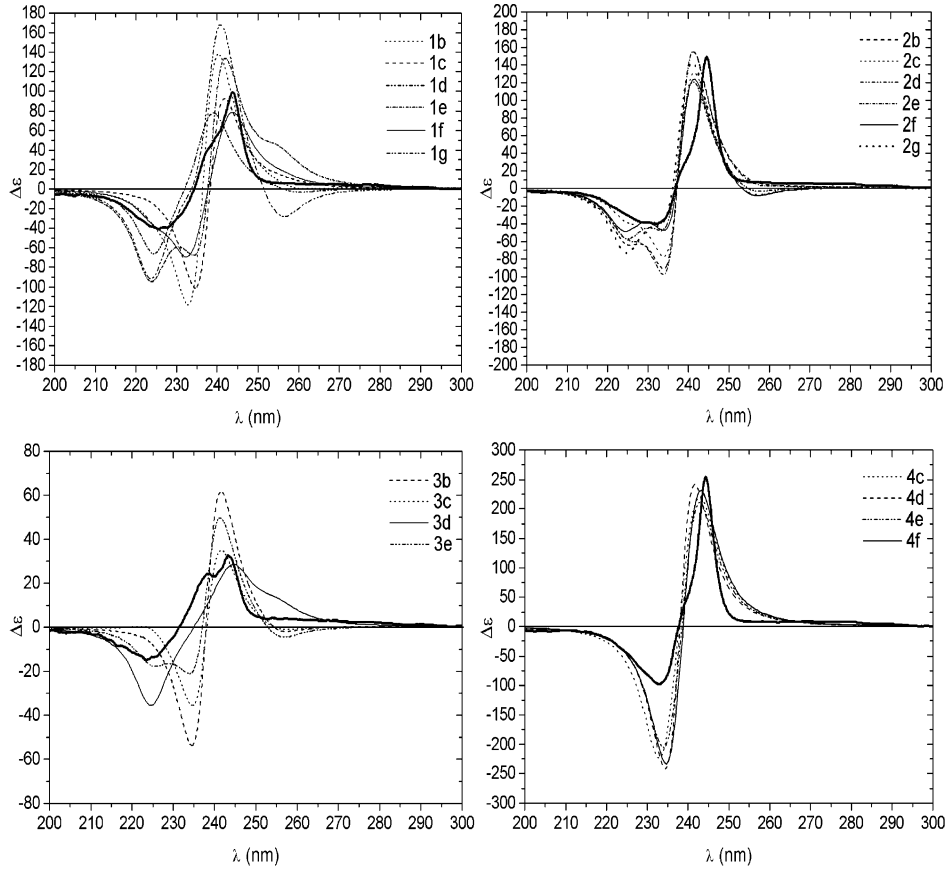

FIGURE 5. Experimental CD spectra of compounds **1**, **2**, **3**, **4** (bold line) and calculated CD spectra of the discarded conformations on the basis of the chosen criteria (see text); ϵ and $\Delta\epsilon$ in mol^{-1} cm^{-1}.

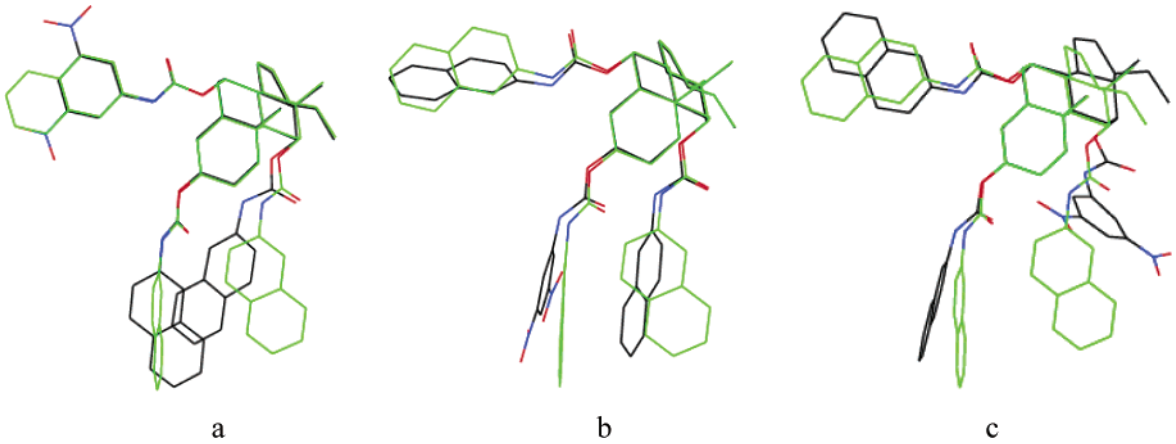

FIGURE 6. Selected minimum energy conformations of compounds **1** (a), **2** (b), and **3** (c), whose theoretical CD spectrum agreed acceptably well with the experimental one, superimposed on the iso-oriented cholestanic backbone to one of the conformations of **4** (drawn in green). For the sake of clarity, hydrogen atoms and the alkyl chain at 17-position are not displayed (for stereoviews, see Figures S9−S11, Supporting Information).

on the iso-oriented cholestanic backbone are also reported.

Molecular Dynamics Simulations

In the hope that a consensus of results is more reliable than results from any single model alone and that the role of solvation on the geometric structure of the compounds under examination could be elucidated, molecular dynamics simulations using AMBER 7[32] with the General AMBER Force Field (GAFF) and HF/6-31G* RESP charges[33] were carried out. Like the traditional AMBER force fields,[34] GAFF uses a simple harmonic

(32) AMBER7: Case, D. A.; Pearlman, D. A.; Caldwell, J. W.; Cheatham, T. E., III; Wang, J.; Ross, W. S.; Simmerling, C. L.; Darden, T. A.; Merz, K. M.; Stanton, R. V.; Cheng, A. L.; Vincent, J. J.; Crowley, M.; Tsui, V.; Gohlke, H.; Radmer, R. J.; Duan, Y.; Pitera, J.; Massova, I.; Seibel, G. L.; Singh, U. C.; Weiner P. K.; Kollman, P. A. University of California, San Francisco, **2002**.

(33) Cornell, W. D.; Cieplak, P.; Bayly, C. I.; Kollman, P. A. *J. Phys. Chem.* **1993**, *97*, 10269−10280.

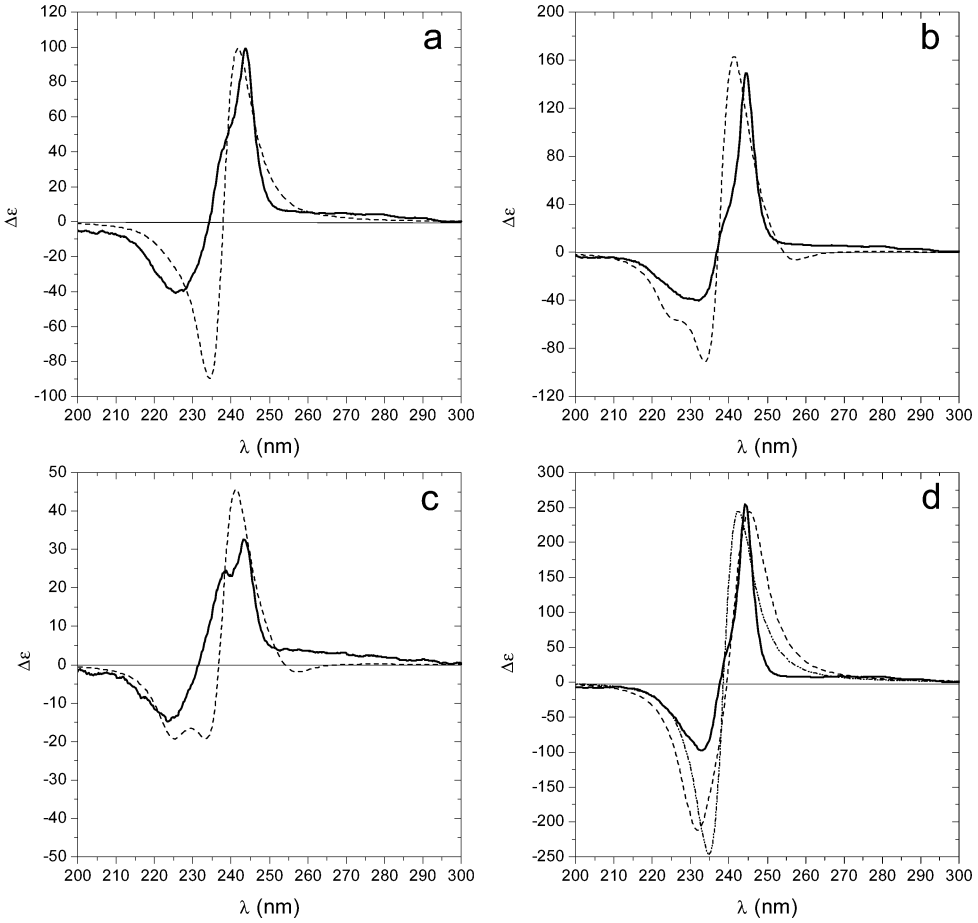

FIGURE 7. Experimental (bold line) and calculated (broken line) CD spectra of compounds **1** (a), **2** (b), **3** (c), **4** (d); ϵ and $\Delta\epsilon$ in mol^{-1} cm^{-1}.

functional form for bonds and angles, but atom types are more general and cover most of the organic chemistry space.

The acetonitrile (MeCN) solvent molecules were represented explicitly using a flexible six-site model for each monomer unit. Parameters for this all-atom model were taken from Howard et al.[35] while the charges were fitted to the electrostatic potential[36] of isolated acetonitrile. There is no conformational variability for acetonitrile that is a linear molecule with an essentially freely rotating methyl group.

Molecular dynamics simulations in acetonitrile solution were carried out, in the NPT ensemble, for solute **2** and 698 solvent molecules in a rectangular parallelepiped box using periodic boundary conditions, a time step of 1 fs and Ewald summations to handle long-range electrostatic interactions. A 12 Å cutoff for nonbonded interactions was applied. The pressure was kept at 1 bar with a coupling constant of 0.1 ps, isothermal compressibility was set to 81.7 (Pa^{-1}),[37] while a dielectric constant $\epsilon = 1$ was employed.

After 5000 steps of energy minimization to remove bad steric contacts, the system was heated under constant volume conditions to 600 K over 10 ps of dynamics, freezing the solute coordinates in order to randomize the positions of solvent molecules. The system was allowed to equilibrate at this temperature for 10 ps, then the temperature was lowered over 10 ps to 300 K. Subsequently, all the constraints were removed and the system was equilibrated for 10 ps. The equilibration continued at constant pressure for 30 ps to bring the artificial box to a reasonable density (∼0.78 g/cm^3).[38] After equilibration, all energetic terms, temperature, volume and pressure turned out to be stabilized and oscillating around their mean values. Thus starting from the last equilibrium configuration obtained, a simulation of ∼5 ns was performed in the NPT ensemble for data collection. During temperature scaling processes, the temperature was adjusted by a fast velocity scaling algorithm, whereas Berendsen's more gentle temperature bath coupling[39] was used during the equilibration and production phases. The pressure adjustment to 1 bar was achieved with an analogous pressure bath coupling. The SHAKE algorithm

(34) (a) Weiner, S. J.; Kollman, P. A.; Case, D. A.; Singh, U. C.; Ghio, C.; Alagona, G.; Profeta, S., Jr.; Weiner, P. *J. Am. Chem. Soc.* **1984**, *106*, 765−784. (b) Weiner, S. J.; Kollman, P. A.; Nguyen, D. T.; Case, D. A. *J. Comput. Chem.* **1986**, *7*, 230−252.

(35) Howard, A. E.; Cieplak, P.; Kollman, P. A. *J. Comput. Chem.* **1995**, *16*, 243−261.

(36) (a) Besler, B. H.; Merz, K. M., Jr.; Kollman, P. A. *J. Comput. Chem.* **1990**, *11*, 431−439. (b) Singh, U. C.; Kollman, P. A. *J. Comput. Chem.* **1984**, *5*, 129−145.

(37) Narayanaswamy, G.; Dharmaraju, G.; Raman, G. K. *J. Chem. Thermodyn.* **1981**, *13*, 327−331.

(38) (a) Gallant, R. W. *Hydrocarb. Proc.* **1969**, *48*, 135−141. (b) Akhmetkarimov, K. A.; Mai, I. I.; Muldakhmetov, Z. M. *Zh. Obshch. Khim.* **1973**, *43*, 458−461.

(39) Berendsen, H. J. C.; Postma, J. P. M.; van Gunsteren, W. F.; DiNola, A.; Haak, J. R. *J. Chem. Phys.* **1984**, *81*, 3684−3690.

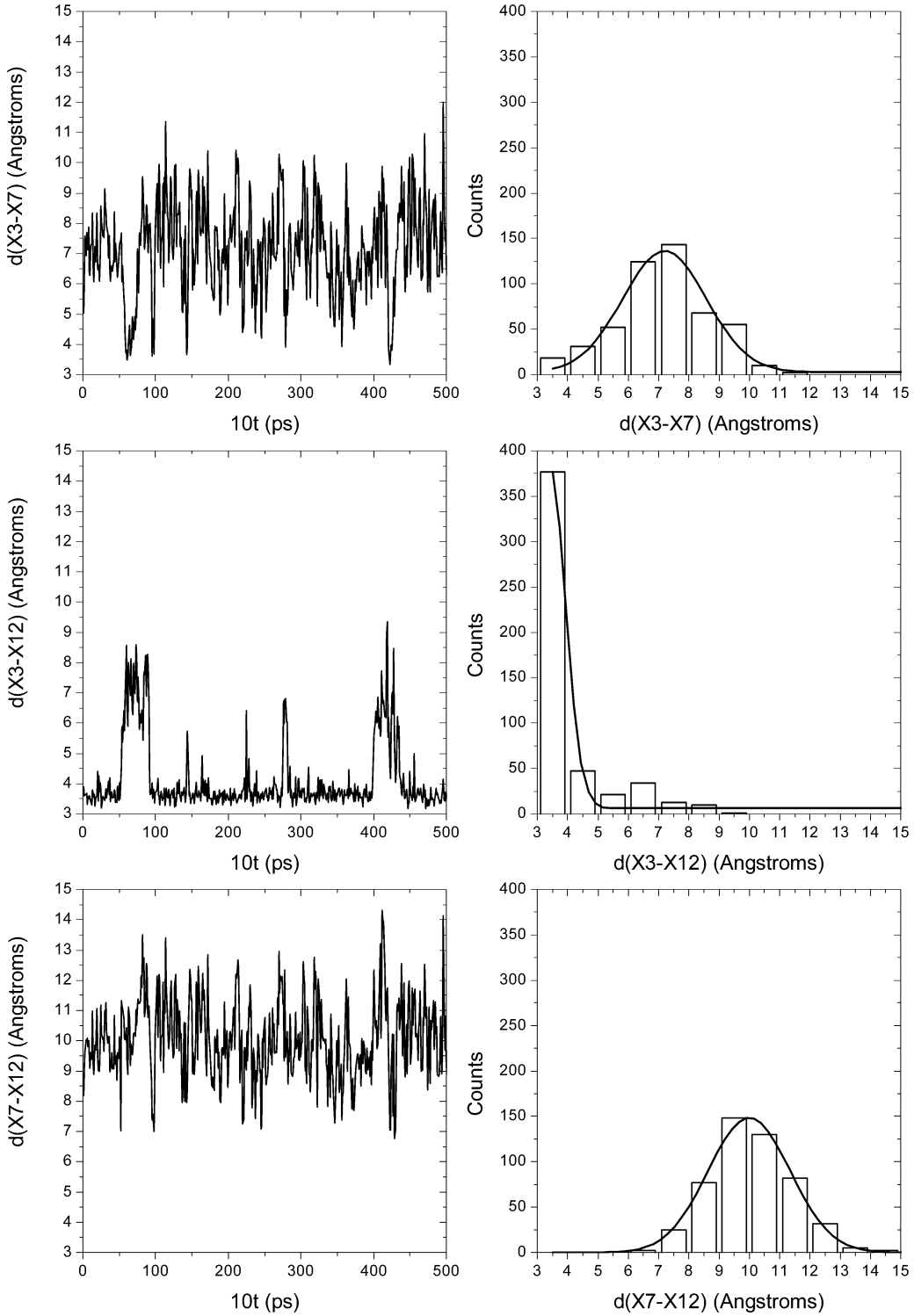

FIGURE 8. Trajectories of the X3−X7, X3−X12, and X7−X12 centroid distances from the 5 ns molecular dynamics simulation carried out for compound **2** in acetonitrile solution at 300 K. The frequency distribution of the conformers is given on the right-hand side of each plot.

was used to constrain all X−H bonds to their equilibrium values. The coordinates were saved every 10 ps to analyze the trajectory.

Since interconversion of different rotamers for side-chains rarely occurs in a simulation at 300 K within 5 ns, the equilibrium rotamer populations cannot properly be estimated from a molecular dynamics trajectory at this temperature. A common practice is to raise the temperature in order to cross over energy barriers and explore more states. However, we are presently interested in structure modifications due to the solvent effect rather than in the thermodynamics of the solvation process.

The distributions of the $\tau_{1,2}$(X) torsional angles apparently reflected relatively stiff conformations without large deviations from the starting geometry: a minimum energy structure whose $\tau_{1,2}$(3), $\tau_{1,2}$(7), and $\tau_{1,2}$(12) dihe-

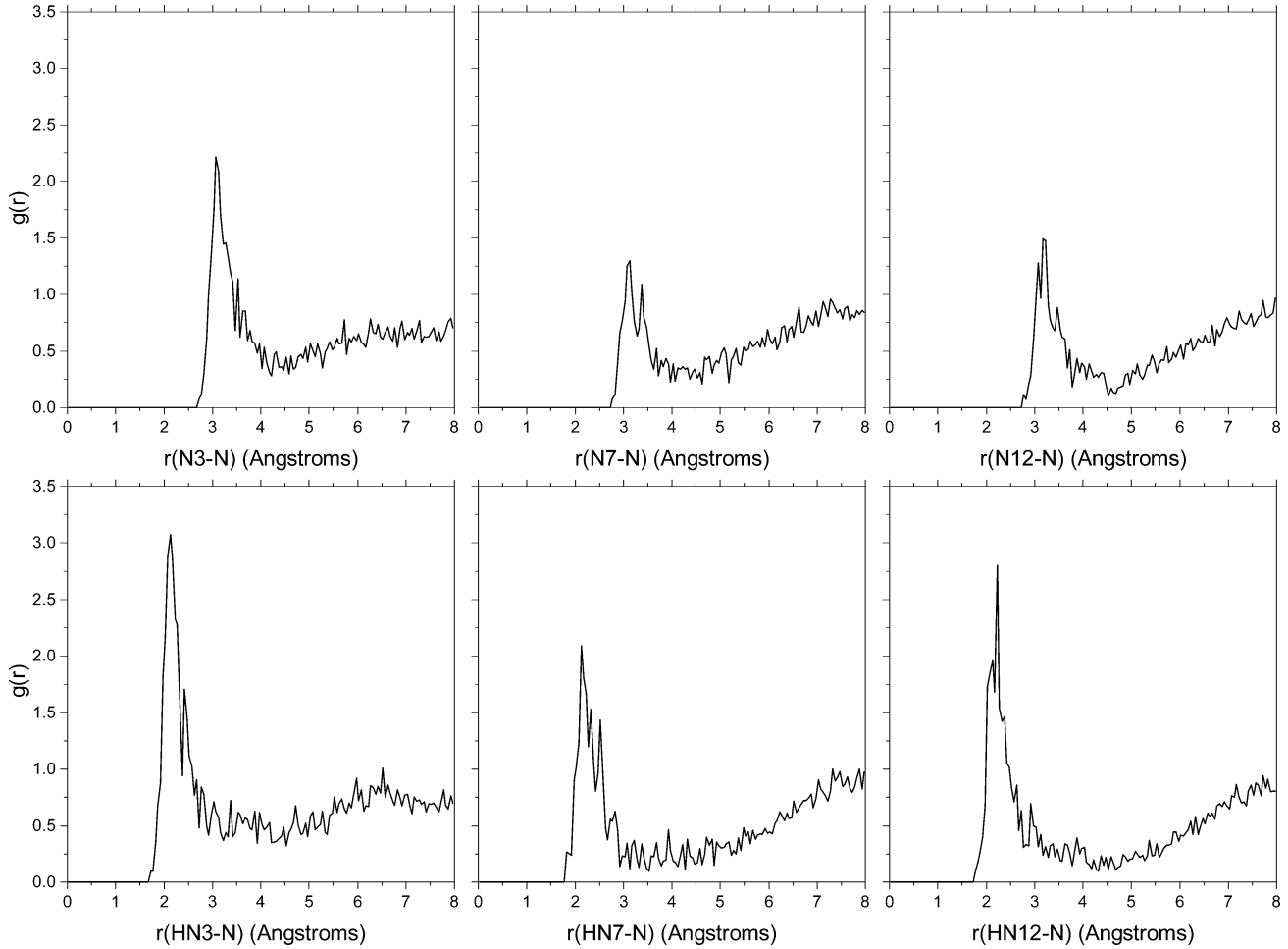

FIGURE 9. Radial distribution functions, *g*(r), from the molecular dynamics simulation of **2** in acetonitrile at 300 K, for N3, N7, N12 atoms and the acetonitrile nitrogen atoms (top) and those for the carbamate hydrogen atoms HN3, HN7, HN12 and the acetonitrile nitrogen atoms (bottom).

drals assumed the (**G**$^+$,**T**), (**G**$^-$,**T**), and (**T**,**T**) pairs, respectively. Nonetheless, the dispositions of the aromatic groups considerably changed.

Analysis of the X3−X7, X3−X12, and X7−X12 centroid distances as a function of time showed that the amplitude of their motion was considerable. In Figure 8, the oscillation of these distances along the whole simulation as well as their distributions are shown.

It is apparent that the X7−X12 and X3−X7 distance fluctuations have a very broad range of variation roughly comprised between 6.8 and 14.3 Å and between 3.4 and 8.6 Å, respectively, whereas the X3−X12 distance fluctuates in the range 3.2−4.2 Å and only occasionally jumps to higher values ($X3-X12_{max} = 9.3$ Å).

The computed atom−atom radial distribution functions (rdfs) around the C-3, C-7 and C-12 carbamate hydrogen and nitrogen atoms, named HN3, HN7, HN12 and N3, N7, N12, respectively, are displayed in Figure 9. As shown, there is no substantial organization of solvent molecules around these hydrogen atoms. The HN12−N(MeCN), HN7−N(MeCN), and HN3−N(MeCN) rdfs exhibit maxima at 2.22, 2.12, and 2.12 Å, respectively, with a coordination number (estimated by integration of the curves) of 1.1, 1.0, and 1.5, respectively, suggesting that one to two acetonitrile molecules are favorably positioned to interact with these polar hydrogens. The almost linear arrangement of the NH groups and the solvent nitrogen atoms can be deduced from the N12−N(MeCN), N7−N(MeCN), and N3−N(MeCN) rdfs, taking into account that an N−H bond is 1.01 Å. This is consistent with HF/6-31G* calculations carried out on a model system (*N*-methylcarbamic acid−acetonitrile) which gave for the optimized adduct geometry a (N)H−N(MeCN) distance of ∼2.3 Å, a N−N(MeCN) distance of ∼3.2 Å, and a ∠NHN angle of ∼163°.

The number of coordinated solvent molecules depends on the NH group orientations. The NH groups can be directed either toward the cholestanic backbone or toward the outside. During the molecular dynamics simulation, actually, the NH group disposition did not substantially change with respect to the initial conformation. Since in **2** the C-3 NH (the H, not shown in Figure 4, is trans with respect to the carbonyl O) is oriented toward the outside of the cholestanic ring, it is more exposed to the solvent and can sometimes interact with two acetonitrile molecules, while the other two NH groups, that are primarily oriented toward the cholestanic ring, could coordinate just a single solvent molecule.

Conclusions

In this paper, we have reported a study of the conformation of the cholic acid derivatives **1**−**4** exploiting a

combined CD-molecular mechanics approach. Using a random assignment of the main dihedral angle values a huge number of conformations was generated and energy refined with two different force fields (Tripos and MMFF94). The structures, grouped in several families according to particular conformational features, turned out to be consistent regardless of the force field used to generate them. Therefore, in the subsequent analysis only those derived from the Tripos force field were considered and the number of conformers was sharply reduced by applying appropriate conformational filters.

Since the molecular mechanics refinements were carried out on the isolated molecules (though making use of a dielectric constant apt to mimic at least in part the solvent screening effect), the possible outcome produced by the presence of real solvent molecules (acetonitrile, in this case) was to be examined. A 5 ns molecular dynamics simulation, carried out in the NPT ensemble on compound **2**, as a test case, revealed frequency distributions centered on the starting structure. Thus, the presence of the acetonitrile molecules did not substantially change the three-dimensional structure, defined by the two torsional angles closest to the cholestanic backbone, obtained using simple continuum models, while it confirmed the mutual flexibility of the aromatic ring systems.

The comparison between experimental and theoretical (calculated by means of the De Voe model) CD spectra has allowed us to characterize those conformations that afforded a satisfactory agreement between experimental and calculated CD data. In addition, the additivity of the contributions of each 2-naphthylcarbamate chromophore to the CD spectrum of compounds **1**−**4** has provided a further criterion to select, among the computed conformations, those in which the 2-naphthylcarbamate moieties are mutually disposed in a similar fashion, as far as the angle between their transition dipole moments is concerned, in the four derivatives. The present study permitted us to exclude that the different enantiodiscriminating behavior exhibited by compounds **1**−**4** is due to a dramatic change of their conformational features in passing from **1** to **4**: actually, the different arrangement of the arylcarbamoyl substituents upon the cholestanic backbone does not engender a different orientation of the aromatic substituents with respect the cholestanic skeleton. On the basis of the present results, it is conceivable that the observed distinct enanatiodiscriminating capabilities are due to the different stereochemical environment of the 3, 7, and 12 positions which is reflected in the different stereodependent interactions produced by the same carbamate moiety depending on the position where it is located upon the cholestanic backbone. Further studies are in progress to ascertain this point.

In general, our study via a combined CD-molecular mechanics approach has proven to be a powerful tool to assess the conformation of complex molecules with several degrees of torsional freedom, containing more than 50 heavy atoms, such as compounds **1**−**4**, which possess, in a chiral rigid structure, chromophores endowed with electrically allowed transitions.

Experimental Section

Circular dichroic spectra were obtained on a JASCO J-710 spectropolarimeter using a 0.1-mm path length cell and spectropolarimetric grade acetonitrile as a solvent, at 25 °C, unless otherwise specified. Sample concentration for CD analyses was typically (6−9) × 10^{-4} M. Ultraviolet−visible absorption spectra were obtained on a Perkin-Elmer Lambda19 spectrophotometer using a 0.1-mm path length cell and spectrophotometric grade acetonitrile as a solvent, at 25 °C. Sample concentration of UV−vis analyses was typically (6−9) × 10^{-4} M.

Molecular mechanics calculations were performed using the SYBYL software[15] with (a) the Tripos force field and Gasteiger−Hückel charges[16] and (b) MMFF94 force field[17] and BCI charges running on SGI Indigo^2 and O^2 workstations. Theoretical excitation spectra were computed using the ZINDO[40] module of the MSI Cerius^2 software[31] running on an SGI O^2 workstation. Molecular dynamics simulations were performed using the AMBER 7 package[32] with the GAFF force field and HF/6-31G* RESP charges.[33] Ab initio calculations were performed using the Gaussian98[41] system of programs running on a DS20E Compaq Alpha workstation.

Materials. Compounds **1**−**4** were prepared as previously described[9] and matched the reported characteristics.[9]

Acknowledgment. The spectroscopic part of this work was supported by MIUR (Progetto Nazionale Stereoselezione in Sintesi Organica: Metodologie e Applicazioni). S.M. is grateful to James W. Caldwell (UCSF) for granting her the use of the AMBER 7 package.

Supporting Information Available: Figures S1−S3, Table S4, and Figures S5−S11. This material is available free of charge via the Internet at http://pubs.acs.org.

JO0267450

(40) Zerner M. C. In *Reviews of Computational Chemistry*; Lipkowitz, K. B., Boyd, D. B., Eds.; VCH: New York, 1991; Vol. 2, pp 313−365.

(41) Frisch, M. J.; Trucks, G. W.; Schlegel, H. B.; Scuseria, G. E.; Robb, M. A.; Cheeseman, J. R.; Zakrzewski, V. G.; Montgomery, J. A., Jr.; Stratmann, R. E.; Burant, J. C.; Dapprich, S.; Millam, J. M.; Daniels, A. D.; Kudin, K. N.; Strain, M. C.; Farkas, O.; Tomasi, J.; Barone, V.; Cossi, M.; Cammi, R.; Mennucci, B.; Pomelli, C.; Adamo, C.; Clifford, S.; Ochterski, J.; Petersson, G. A.; Ayala, P. Y.; Cui, Q.; Morokuma, K.; Malick, D. K.; Rabuck, A. D.; Raghavachari, K.; Foresman, J. B.; Cioslowski, J.; Ortiz, J. V.; Baboul, A. G.; Stefanov, B. B.; Liu, G.; Liashenko, A.; Piskorz, P.; Komaromi, I.; Gomperts, R.; Martin, R. L.; Fox, D. J.; Keith, T.; Al-Laham, M. A.; Peng, C. Y.; Nanayakkara, A.; Gonzalez, C.; Challacombe, M.; Gill, P. M. W.; Johnson, B. G.; Chen, W.; Wong, M. W.; Andres, J. L.; Head-Gordon, M.; Replogle, E. S.; Pople, J. A. *Gaussian 98*, revision A.7; Gaussian, Inc.: Pittsburgh, PA, 1998.